ISTITUTO NAZIONALE DI FISICA NUCLEARE - ISTITUTO NAZIONALE DI FISICA NUCLEARE - ISTITUTO NAZIONALE DI FISICA NUCLEARE - ISTITUTO NAZIONALE DI FISICA NUCLEARE - ISTITUTO NAZIONALE DI FISICA NUCLEARE - ISTITUTO NAZIONALE DI

Laboratori Nazionali di Frascati

LNF- 89/045(R)
30 Giugno 1989

M. Anghinolfi, N. Bianchi, P. Corvisiero, E. De Sanctis, S. Frullani, F. Garibaldi, G. Gervino, C. Guaraldo, P. Levi Sandri, V. Lucherini, V. Muccifora, E. Polli, A.R. Reolon, G. Ricco, M. Ripani, P. Rossi, M. Sanzone, M. Taiuti, M.G. Urciuoli, A. Zucchiatti:

PROPOSAL OF MEASURING THE TOTAL PHOTONUCLEAR CROSS SECTION BETWEEN 300 MeV AND 1.2 GeV

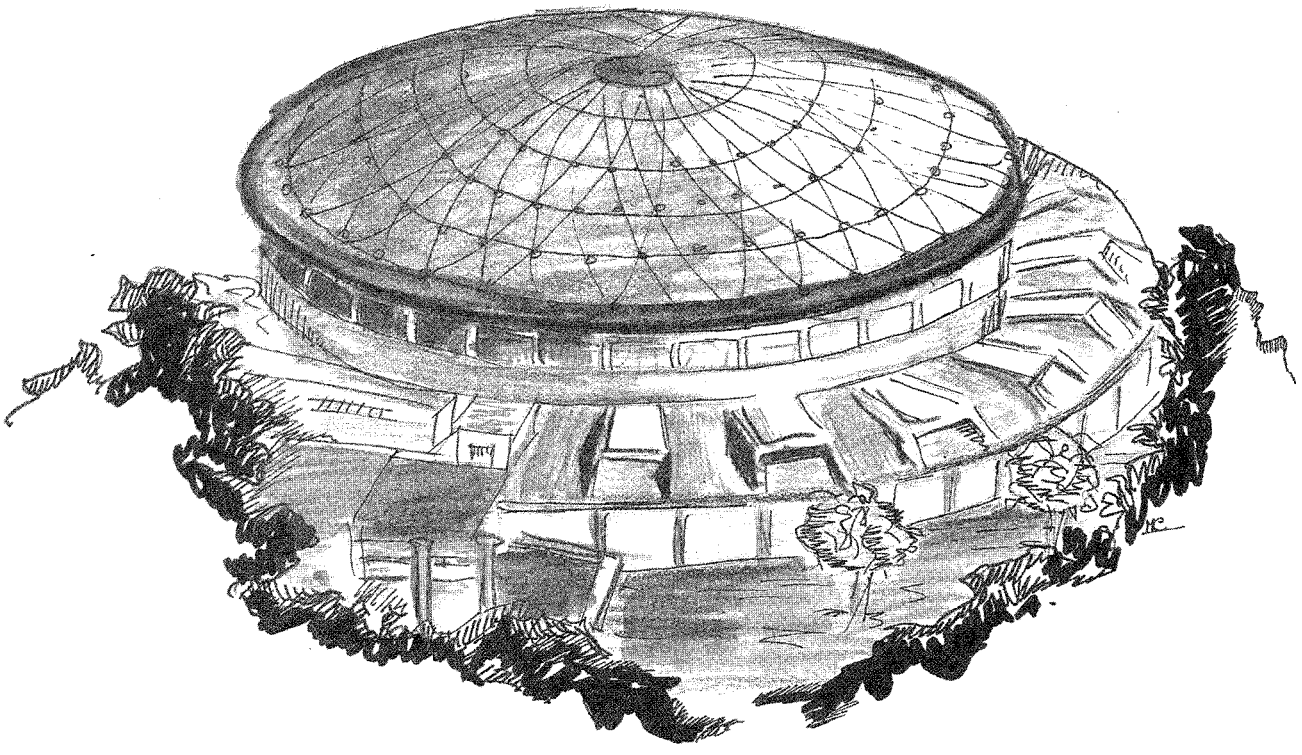

Servizio Documentazione
dei Laboratori Nazionali di Frascati
P.O. Box, 13 - 00044 Frascati (Italy)

INFN - Laboratori Nazionali di Frascati
Servizio Documentazione

LNF-89/045(R)
30 Giugno 1989

PROPOSAL OF MEASURING THE TOTAL PHOTONUCLEAR CROSS SECTION BETWEEN 300 MeV AND 1.2 GeV

M. Anghinolfi[1], N. Bianchi[0], P. Corvisiero[1], E. De Sanctis[0], S. Frullani[2], F. Garibaldi[2], G. Gervino[3], C. Guaraldo[0], P. Levi Sandri[0], V. Lucherini[0], V. Muccifora[0], E. Polli[0], A.R. Reolon[0], G. Ricco[1], M. Ripani[1], P. Rossi[0], M. Sanzone[1], M. Taiuti[1], M.G. Urciuoli[2], A. Zucchiatti[1]

[0]INFN - Laboratori Nazionali di Frascati, I-00044 Frascati
[1]INFN - Sezione di Genova e Dipartimento di Fisica dell'Università, Genova
[2]INFN - Sezione Sanità e Laboratori di Fisica dell'Istituto Superiore di Sanità, Roma
[3]INFN - Sezione di Torino e Dipartimento di Fisica dell'Università, Torino

ABSTRACT

The new monochromatic photon beam produced by tagging the bremsstrahlung photons radiated on the Argon Jet Target by the electrons circulating into the ADONE storage ring offers the opportunity to measure the total photonuclear cross section in the energy range between 300 MeV and 1200 MeV. In this region, in which only few data exist in literature, it is possible to study the behavior and propagation of nucleonic resonances in nuclear matter and the onset of the hadronic fluctuations of the photon. In this paper we describe the proposed techniques and an experimental apparatus to measure this quantity in a wide range of atomic numbers.

INTRODUCTION

The total photonuclear cross section $\sigma_T(k,A)$, where k is the photon energy and A the target atomic number, is an interesting quantity because combines the limits of the inelastic electron scattering "photon point" (very low transferred momentum) to the forward amplitude for elastic photon scattering (optical theorem) and provides informations on general model

independent properties of the photon-nucleus interaction like the Giant Dipole Resonance (G.D.R.), Sum Rules, nucleonic correlations and mesonic exchange currents, presence of isobaric resonances, hadronic fluctuations of the photon.

To better clarify this point, let us consider the behavior of $\sigma_T(k,A)$ in different photon energy domains.

a) In the energy range up to 140 MeV, that is below the opening of the pion photoproduction channel, the total photonuclear cross section shows a broad resonance for all nuclei (GDR), centered at ≈15-20 MeV; this fact clearly reveals the collective modes of excitations of nuclei.[1] Moreover, it is possible to compare the measured $\sigma_T(k, A)$ with the theoretical previsions based on general properties of the interactions of the electro-magnetic (e.m.) field with charged particles. Typical, to this respect, is the classical dipole sum rule of Thomas-Reich-Kuhn (TRK), which gives for a photon interacting with an ensemble of elementary charges (as a nucleus with A, Z and N=A-Z, nucleons, protons and neutrons, respectively) the well known result:

$$\Sigma_0 \equiv \int_0^\infty \sigma_T(k,A)\, dk = 60 \frac{NZ}{A} \text{ MeV mb.} \qquad (1)$$

Measurements of $\sigma_T(k, A)$ made at Mainz[2] and Saclay[3] with different techniques on different nuclei showed that this integral on photon energy up to m_π exceeds the TRK result by a factor $(1+k)$, with k, *enhancement factor*, ranging from 0.5 to 1 (Fig.1). This finding shows the relevance of meson exchange currents in nuclei: in fact, in the Long Wave Approximation, Σ_0 is directly proportional to the double commutator $\langle 0|[D_z,[H,D_z]]|0\rangle$, where $|0\rangle$ is the nuclear ground state, H the nuclear Hamiltonian, and D_z the z component of the electric dipole operator. The explicit development of the double commutator shows that the enhancement factor k is proportional to the commutator $\langle 0|[D_z,[V,D_z]]|0\rangle$, where V is the nuclear potential. If V does not contain exchange contributions (momentum dependent) k should be zero. This interpretation has been recently pushed forward by T.A. Arakelyan, L.S. Davtyan and S.G.Mitinyan,[4] which ascribe the enhancement factor to the quark substructure of nucleons (the truly elementary charges) and to the probability of production of six-quark clusters in the nucleus.

b) For energies between 140 MeV and 450 MeV, region of the Δ resonance, the data on $\sigma_T(k, A)$ obtained by various laboratories (Mainz,[5,6] Saclay,[5,7,8] Bonn,[5,9] Frascati[10]) on different nuclei using different techniques show that this quantity is proportional to the number A of nucleons, indicating a *volume like* absorption. This result allows to define, in this energy region, a *universal curve* for the photonuclear absorption valid for all nuclei and given by the ratio of $\sigma_T(k, A)$ to the total number of nucleons (Fig.2): the photon counts all nucleons, each acting as an incoherent absorber.

c) In the energy region from 450 MeV up to ≈2 GeV, it exists only one measurement on light and medium heavy nuclei (Be, C, Al, H_2O and Cu), made at Erevan with a tagged bremsstrahlung beam.[11] Unfortunately these data were collected with large acceptance over the actual photon energy and fluctuate well above the experimental errors (Fig.3). When one takes their mean value, normalized to A, two facts seem to emerge: i) the smearing of the nucleonic resonances at ≈700 MeV and ≈1 GeV clearly seen in the photoabsorption on proton and deuteron; ii) the onset, already at ≈1100 MeV, of the shadowing effect (Fig.4). It is worth to note, however, that more recent experimental data on electrofission of ^{238}U measured at low Q^2 by the same authors[12] do not show any shadowing effect from 1 GeV up to 3.2 GeV.

d) In the high energy region, from 2 GeV up to 180 GeV,[13] the measurement of $\sigma_T(k,A)$ can give informations on the hadronic fluctuations of the photon (Vector Dominance Model) that produce the shadowing effect: the photon has a finite probability to convert into a vectorial meson (like the ρ), interacting strongly with the nucleus. Hence $\sigma_T(k, A)$ is no more proportional to the number A of the nucleus, but it is equal to the product of $\sigma_T(k)$ on free nucleon times A_{eff}, being $A_{eff}=A^{\alpha}$. The present experimental data (Fig.5) suggest a value $\alpha\approx0.9$, intermediate between a volume absorption, $\alpha=1$, typical of an e.m. probe, and a surface absorption, $\alpha=2/3$, typical of a hadronic probe.

This analysis indicates that the photon energy region between the real pion production threshold and 1÷2 GeV is still open to interesting questions.

The new tagged photon beam produced on Argon condensed jet installed on the ADONE storage ring will span the energy region between 200 MeV and 1200 MeV,[14] just covering this interesting physical region. In the following paragraphs a proposal is presented to measure with this photon beam the total photonuclear cross section on light and heavy nuclei.

THE JET TARGET TAGGED PHOTON BEAM

The photon beam is produced by bremsstrahlung of the electrons circulating in the ADONE storage ring of the Frascati Laboratories on an internal target consisting of a molecular Argon beam crossing, at supersonic speed, the ring vacuum pipe in straight section N.5.[14] This target (Jet Target) is thin enough (≈10^{-10} l.r.) to not degrade the circulating beam quality, assuring several minutes of beam lifetime.

The Argon jet target consists of three parts: i) the jet injection system, where the jet is produced with the help of a special trumpet-shaped nozzle and several orifices; ii) the interaction chamber, where the molecular jet crosses the electron beam at about 25 cm from its source point; iii) the jet dump, which has to ensure that the jet is pumped away without significant backstreaming. Three differential pumping stages have been interposed to separate both the jet-injection and jet-dump chambers from the vacuum pipe in order to minimize

pressure rise in the interaction region. Each room between two successive orifices is pumped on by a 360 l/s turbomolecular pump, which is directly flanged to the relevant vacuum chamber, while both the expansion and sink chambers are evacuated by a high speed (1000 l/s) turbomolecular pump. Two fast acting UHV valves separate the production and sink chambers from the ADONE vacuum pipe to easy the jet on/off operations and to prevent the possible contamination of the ring in case of a large pressure bump due to breakdown of the target system. The operation of the target are controlled by a microprocessor-based system which performs all tasks to start up the jet on/off procedure, recording all the parameters, and safety checks. The operating conditions are: inlet pressure and temperature 1÷20 bar and about 300 °K, respectively; nozzle throat diameter 87 μm and semiaperture 3.5°. From a total flux of $\approx 10^{20}$ Ar-atoms/s expanding from the nozzle, the collimator system selects about 10^{17}÷10^{18} atoms/s, which corresponds to a target thickness of 1÷10 ng/cm^2 (∅=6 mm) on the path of the electron beam.

The recoil electrons are momentum analyzed by the next ADONE bending magnet and detected by a two arrays of scintillation counters in coincidence (39 counters each array). This hodoscope is placed between the ring vacuum pipe and the magnet flux return joke. The scintillators define 76 energy channels and have different sizes in order to give a constant photon energy resolution (1%, for electrons of E_{e^-}=1500 MeV, and 2.7% for E_{e^-}=500 MeV) over the whole tagging range $\Delta k = (0.4 \div 0.8)\ E_{e^-}$. Each scintillator is connected to its phototube by means of optical fibers. The intensity of photons will be, under normal operating conditions (circulating electron current ≈60 mA and jet thickness 5 ng/cm^2), of $\approx 10^7$ photons/sec over the whole tagging range.

I) TOTAL PHOTONUCLEAR CROSS SECTION ON LIGHT NUCLEI

A convenient method of measuring the total photonuclear cross section on light nuclei is the transmission method: the total photonuclear cross section is obtainable subtracting the large atomic e.m. contribution, which, for light nuclei, is minimized ($\approx Z^2/A$ behavior of the ratio atomic/nuclear cross sections) and computable with good accuracy.[15] Schematically, it consists of an intensity photon monitor, an absorption target, and a photon spectrometer: it is necessary to measure, for a given photon energy bin, the normalized number of photons which reach the spectrometer with the absorber In and Out the beam. If $N_{Out}(k)$ and $N_{In}(k)$ are the detected number of photons of energy k, normalized at the same unit of monitor, with, respectively, target Out and In, we have:

$$N_{In}(k) = N_{Out}(k) \cdot exp[-(\mu_N + \mu_{At})t] \quad , \qquad (2)$$

where t is the target thickness, μ_N, μ_{At} are, respectively, the nuclear and atomic absorption

coefficients, and $\mu_{N(At)}=\sigma_{T(At)}\cdot\mathcal{N}\,\rho/A$, being $\mathcal{N}$ the Avogadro number, and ρ and A the target density and atomic number, respectively. Inverting eq.2, we obtain:

$$\sigma_T(k,A) = \frac{A}{\mathcal{N}\rho t}\ln\left(\frac{N_{Out}(k)}{N_{In}(k)}\right) - \frac{A}{\mathcal{N}\rho}\mu_{At}\,. \qquad (3)$$

To use eq.3, it is necessary to reduce as much as possible the contribution to $N_{In}(k)$ due to the secondary particles of the e.m. shower produced by the primary photons in the absorber. This will be achieved, first of all, requiring coincidence of the photon detector with a specific channel of the Tagging system, so that the energy balance relation ($k=E_{e^-} - E'_{e^-}$) is overdetermined: this ensures also a big suppression of systematic errors arising from fluctuations in detectors response. Moreover, the overall cleanness of the transmitted beam can be improved with a proper choice of the geometric configuration of the experiment: a long distance between the absorption target and the photon detector, and a larger angular divergence of the shower particles with respect to that of the primary photon beam will assure a minimal contamination of the transmitted photon beam. To further minimize the shower background on the photon detector, the absorber will be totally inserted inside a uniform magnetic field (≈12 kG). In fact, a Monte Carlo simulation of the shower produced by a bremsstrahlung beam of maximum energy ≈1 GeV crossing the absorber showed that this configuration is the cleanest one, since it increases the angular divergence of the shower particles, sweeping them from the primary photon beam. This can clearly be seen in Fig.6, where it is shown the spectrum of secondary particles reaching the detector for a primary bremsstrahlung beam of head energy 1 GeV crossing a 60 cm thick C target. Nevertheless, some of the shower energy still reaches the photon detector, giving rise to a low energy tail (*build-up* phenomena): this means that, for each electron energy E_{e^-}, there is a minimum photon energy below which the transmitted spectrum may be contaminated. From the Monte Carlo calculation, the "safe" region results to lay above $\approx 0.6E_{e^-}$.

Being the "good" signal only 1%÷2% of the measured quantities, in this type of experiment it is essential to keep the statistical errors on the measured spectra $N_{Out}(k)$ and $N_{In}(k)$ as low as 0.1%. In this way, eventual resonances in the cross section will not be masked by statistical fluctuations.

The statistical errors are strongly dependent, for a given photon intensity and total time of measurement, upon the target thickness and the adopted technique of measurement. If, as usual, the primary beam intensity is kept constant, both with the absorber In and Out, the statistical error on $\sigma_T(k, A)$ has a decreasing-increasing behavior as the target thickness increases. If, on the contrary, the intensity of the beam on the detector is kept constant (for instance with a proper modulation of the jet beam density), both with absorber In and Out, the statistical error always decreases with target thickness. In both cases, large target thickness

are needed (≈50 cm for light nuclei) to have 5%÷10% statistical error on $\sigma_T(k,A)$. This behavior is clearly seen in Fig.7, where it is shown the quantitative results for the statistical errors in the two possible working conditions derived applying the error propagation rule to eq.3.

The sources of systematic errors are: the target thickness and density, and the atomic electromagnetic cross section to be subtracted: all these quantities must be known at the ≈0.1% level. Moreover, the countings of the monitor which serves to normalize each BGO spectrum must also be stable at the ≈0.1% level.

As photon spectrometer, BGO crystals have been selected: their high density and short radiation length (7.1 g/cm^3 and 1.1 cm, respectively) allow the construction of a compact detector to be built, with high energy resolution (≈3%) and efficiency (≈1) up to the maximum energy of the Jet Target beam (1.5 GeV). The less scintillation efficiency of BGO with respect NaI crystals is not a problem due to the high quantity of light created by the absorption of the high energy photon beam, while its decay time constant is only slightly longer (300 ns instead of 230 ns, respectively).

The spectrometer consists of four cylindrical BGO crystals, aligned one behind the other, each 9.8 cm in diameter and 8 cm in length, giving a total thickness of 29 radiation lengths (shower rear leakage <1%). The diameter is sufficient to transversely contain the 96% of the shower energy for a 2 cm photon beam diameter. Each BGO is seen by three couples of Philips XP 2012B phototubes, with Ø=32 mm, at 120° each from the other. BGO crystals are surrounded for their overall length by a NaI cylindrical ring, divided in three slices of radial depth 15 cm, each seen by three Hamamatsu R1652 phototubes with Ø=75 mm: it can be used to measure the shower energy transversely escaping, so improving the resolution of the BGO's. In Fig.8 a drawing of the photon detector is given, along with its calculated response function for 1 GeV photons. In order to eliminate the cosmic ray background, the BGO+NaI spectrometer will be in anticoincidence with a 5x60x60 cm^3 upper plastic scintillator. The detector will be shielded in all directions by at least 10 cm of Pb walls, while the photon beam will enter the detector through a hole of Ø= 100 mm in a Pb wall 20 cm thick. To minimize possible fluctuations of the detector response function, the four central crystals are kept at a constant temperature while three leds mounted on each BGO monitor gain variations of phototubes.

Due to its high resolution and efficiency, this photon detector will be also used as standard monitor of the Jet Target photon beam at low intensity. The detector, with its shielding, thermostat and electronics, is mounted in the experimental hall on a movable platform, with remote control, that allows its insertion In or Out the photon beam: in Fig.9 the detector mounted in the experimental hall on the movable platform, with the shielding removed, is shown.

Since BGO (and NaI) crystals have a rather long decay constant, care will be paid in avoiding "pile-up" effects which would distort the measured spectrum at high photon beam intensity. An accurate calculation shows that, in order to keep pile-up effects within few percent level, the overall photon intensity lower than $\approx 5\ 10^3$ gamma s^{-1} of tagged photons must be used. This can be seen in Fig.10, where it is shown the fractional pile-up of the bremsstrahlung spectrum of 980 MeV maximum energy, for different beam intensities. Quite the same counting rate limit is achieved when considering both the dead time in data acquisition and the ratio of the anode to voltage divider current. In the former case, if a 10 μs conversion time per true event is assumed, a 1%÷2% dead time is obtained for 10^3 tagged photons. To keep the phototube gain stable within 1% when measuring a continuous luminous flux, the divider current should be at least ten times the anode current: using the already determined photon flux, this limit is easily verified. As a final result, a total tagged photon intensity of $\approx 10^3$ s^{-1} ensures a proper operation of the detector and a suitable acquisition system handling, while keeping the measuring time and the statistical errors reasonably low.

In Fig.11, it is shown a schematic drawing of the experimental facility. The photon beam, produced on the Argon Jet Target (JT) by the electrons circulating in ADONE, leaves the ring vacuum chamber (VC), crosses a wire chamber that allows the beam profile measurement (W1), and is collimated by a lead collimator (C1), ∅=9 mm 20 cm thick, inserted inside the gap of a sweeping magnet (M1), then it crosses the absorption target (T), a 10x10x60 cm^3 reactor graphite, put ≈1 m downstream the collimator, inside the gap of a cleaning magnet (M2). The absorption target can be inserted In or Out the beam by a remotely controlled system: when the absorber is Out, a 60 cm long cylinder (∅=100 mm), hold under vacuum, is inserted on the beam to avoid contamination from the 60 cm of air. Following the target, still inside the magnet, a 20 cm thick lead collimator (C2, ∅=250 mm) cleans from the primary beam the secondary shower particles without intercepting the primary beam. After the M2 magnet, a 15 m long vacuum line (∅=80 mm) transports the photon beam up to the BGO detector, placed in the new Jet Target Experimental Hall, outside the ADONE building, from which it is separated by a 1 m concrete wall. The beam spot on the detector has a FWHM of ≈15 mm. The circulating electrons which have produced the bremsstrahlung photons striking the Jet Target are momentum analyzed by the next ADONE bending magnet (B1) and detected by the tagging counters (TC) put in its gap.

All anode signals of the BGO phototubes will be linearly summed: the resulting signal will be split in two parts: one to drive the logic, the other for linear analysis. To this end a Lecroy FERA ADC will be used, due to its low conversion time. The gate for the ADC analysis will be given by the OR signal of the tagging channels in coincidence with the spectrometer signal, and, for each gate, the pattern configuration of the tagging system will be also read through Coincidence Registers to identify the corresponding tagging channel. The

events will be stored in the memory of a Lecroy CAB module, that enables handling high acquisition rates, and will be organized in a matrix, with columns the ADC signal channels and rows the corresponding tagging channels.

The (summed) signal from the NaI crystals can be used to drive the gate in anticoincidence to increase the energy resolution of the spectrometer.

The overall response of this photon detector has been checked during the first experimental runs with the jet target tagged photon beam. In Fig.12a, it is shown a bremsstrahlung spectrum measured "in single" by the BGO spectrometer. When the ADC analysis of the BGO is gated by one of the tagging channel, a clean peak emerge at the correct channel-energy position, with narrow resolution: ≈3%, as it can be seen in Fig.12b. Measuring the BGO spectrum in single and in coincidence with one tagging channel, for different ADONE electron energies, it has been checked the linearity of the response of the spectrometer in a wide energy range: the result obtained is shown in Fig.13: as can be seen the linear pattern clearly emerges from the data. Using this correspondence channel energy, the calculated bremsstrahlung spectra have been compared to the measured ones: this is shown in Fig.14, where a pretty good agreement between theory and experiment can be seen. The calculated spectra are obtained by means of a shower Monte Carlo code, that takes into account the actual geometry of the experiment.[16] The shown spectra are with absorber Out: it is essential that the photon peak coming from the coincidence with one tagging channel with absorber In maintains the same cleanness: the result is shown in Fig.15: the part a) refers to the case "absorber Out", the part b) to "absorber In". The similarity between these two spectra is a guaranty of the good overall disposition of the experimental apparatus.

II) TOTAL PHOTONUCLEAR CROSS SECTION ON HEAVY NUCLEI

To determine the A dependence of $\sigma_T(k, A)$, a wide range A has to be spanned. As said, the transmission method is feasible only with low A targets. To study the absorption on heavy nuclei, one can use those nuclei whose fissibility (the ratio of the fission cross section to the total inelastic cross section) is ≈1, like Uranium. In fact, in this case, a measurement of the photofission cross section is equivalent to the measurement of the total photoabsorption cross section. This method has already been applied up to k=450 MeV to measure the total photoabsorption cross section of ^{235}U and ^{238}U.[7,12] To extend this measurement at higher energies (≈1 GeV), one must be sure that the Uranium fissibility keeps equal to ≈1: this seems to be the case, according to theoretical calculations of A.S Iljinov and M.V. Mebel.[17] This type of technique is then proposed for the measurement of $\sigma_T(k, A)$ on heavy nuclei with the jet target tagged photon beam.

The fission fragments are very ionizing "particles", and this large ionization is a clear signal of the fission event. To choice the fission detector, one has to consider the following: a

very thin target is necessary, to allow fission fragments to escape (typical fission fragment range in Uranium is ≈8 mg/cm^2). Hence, to compensate for the consequent low counting rate, a large solid angle detector is necessary. Moreover, the fission fragment detector must be "active" and fast enough (≈1 ns) to be used in coincidence with the tagging counters to associate the corresponding photon energy.

A suitable fission detector satisfying the above requirements is the Parallel Plate Avalanche Detector (PPAD). In Fig.16, a schematic drawing of a PPAD is given. The PPAD is, in practice, a parallel plate ionizing chamber, working in proportional regime: its geometry ensures a solid angle ≈4π, and its efficiency is ≈1. The used gas can be isobutane at a pressure of few torrs. The gap between plates is small (3 mm), which ensures an intrinsic fast response (≈100 ps). The target, deposited directly on the inner surface of one plate, will have a thickness of ≈ 2 mg/cm^2. By properly selecting the working conditions, it is possible to put the detector directly of the photon beam, without being disturbed by it and the shower particles. Moreover, it is possible to put many detectors one behind the other to increase the total counting rate: to this end, the plate thickness must be thick enough to stop the fission fragments and avoid "double counting" problems, and thin enough not to affect the photon beam. A thickness ≈50 μm of Al will be appropriate for the aims. The absolute calibration of the detector will be easily achieved by using spontaneously fissioning nuclei as ^{252}Cf, and also Monte Carlo techniques. A special double PPAD chamber, with a central target of very thin thickness (0.3 mg/cm^2), in order to detect in coincidence both fission fragments, can also be used for absolute calibration, while a similar ones without target can serve as background monitor.[18]

With a pile of 60 PPAD, each with 2 mg/cm^2 U target, detection efficiency ≈1 and 10^3 photons s^{-1} for each tagging channel, ≈50 fission counts per hour and per tagging channel are expected at k≈700 MeV, which means a ±5% statistical error on the total cross section in about one day of measurement.

With this type of detector, even if the target fissibility will abruptly drop at high photon energy, due to the onset of multifragmentation phenomena, it would be possible to detect the fragment's ionization and, hence, the photonuclear event.

REFERENCES

1) R. Bergere, in Photonuclear Reactions I, Lecture Notes in Physics **61**, p.1, Springer Verlag (1977), ed. by S.Costa and C.Schaerf.
2) J. Ahrens *et al.*, Nucl. Phys. **A251**, 479 (1975).
3) A. Lepretre *et al.*, Nucl. Phys. **A367**, 237 (1981).
4) T.A. Arakelyan *et al.*, Sov. J. Nucl. Phys. **49**, 55 (1989).
5) J. Ahrens *et al.*, Phys. Lett. **146B**, 303 (1984).
6) B. Ziegler, in Nuclear Physics with Electromagnetic Probes, Lecture Notes in Physics **108**, p.148, Springer-Verlag (1979), ed. by H Arenhovel and D. Drechsel.
7) M.L. Ghedira, Proceedings 8ème Session de Physique Nucleaire Aussois, S. 9-1 (1985).
8) P. Chollet *et al.*, Phys. Lett. **127B**, 331 (1983).
9) J. Arends *et al.*, Phys. Lett. **98B**, 423 (1981).
10) V. Bellini *et al.*, Il Nuovo Cimento **85A**, 75 (1985).
11) E.A. Arakelyan *et al.*, Sov. J. Nucl. Phys. **38**, 589 (1983).
12) E.A. Arakelyan *et al.*, Sov. J. Nucl. Phys. **49**, 780 (1989).
13) T.H. Bauer *et al.*, Rev. Mod. Phys. **50**, 261 (1978) and references therein.
14) E. De Sanctis *et al.*, Few Body Suppl. 1, p.414 (1986) and Frascati Report LNF-90/01(P), in press.
15) J.H. Hubbell *et al.*, J. Phys. Chem. Ref. Data **9**, 1023 (1980).
16) P. Corvisiero *et al.*, Nucl. Instr. & Meth. **185**, 291 (1981) and **211**, 135 (1983).
17) A.S. Iljinov and M.V. Mebel, private communication.
18) P. Garganne, Saclay Note CEA-N-2492 (1986).

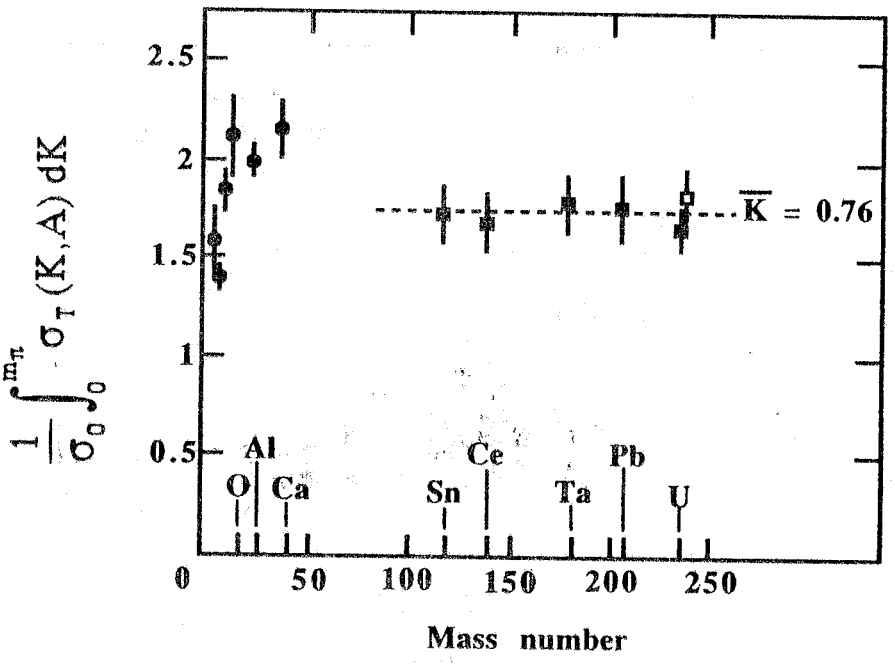

FIG. 1 - Total photonuclear cross section $\sigma_T(k, A)$, integrated in k up to the photopion production threshold m_π, in unit of σ_0, the classic TRK value of the Dipole Sum Rule (results of Mainz,[2] full circles, and Saclay,[3] open and full squares).

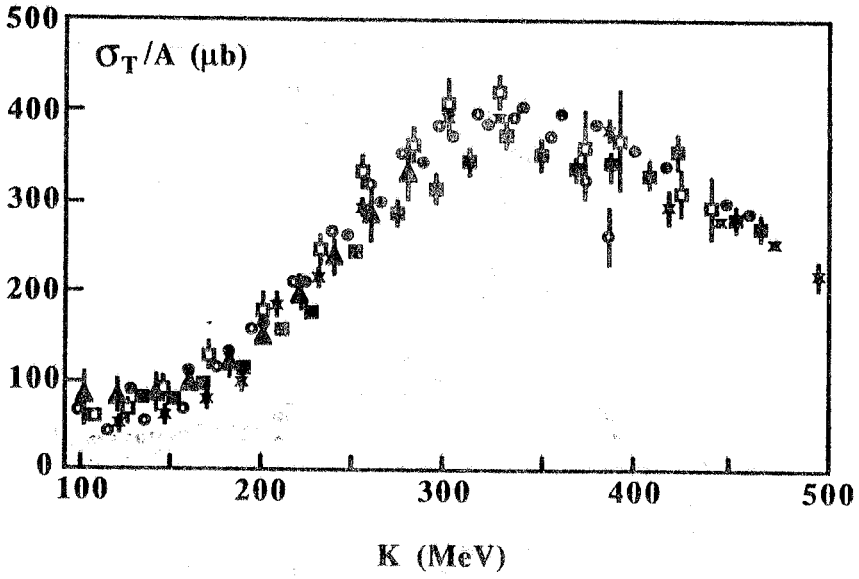

FIG. 2 - Total photonuclear cross section per nucleon, $\sigma_T(k, A)/A$, as a function of photon energy k, from pion photoproduction threshold up to ≈500 MeV, measured with different techniques, at various Laboratories on different nuclei: full triangles, ^{238}U (Frascati)[10]; open circles, ^{9}Be (Bonn)[9]; crosses, ^{12}C, and open squares, ^{208}Pb (Saclay)[7,8]; full squares, ^{235}U, and full circles, ^{238}U (Bonn-Mainz-Saclay collaboration)[5].

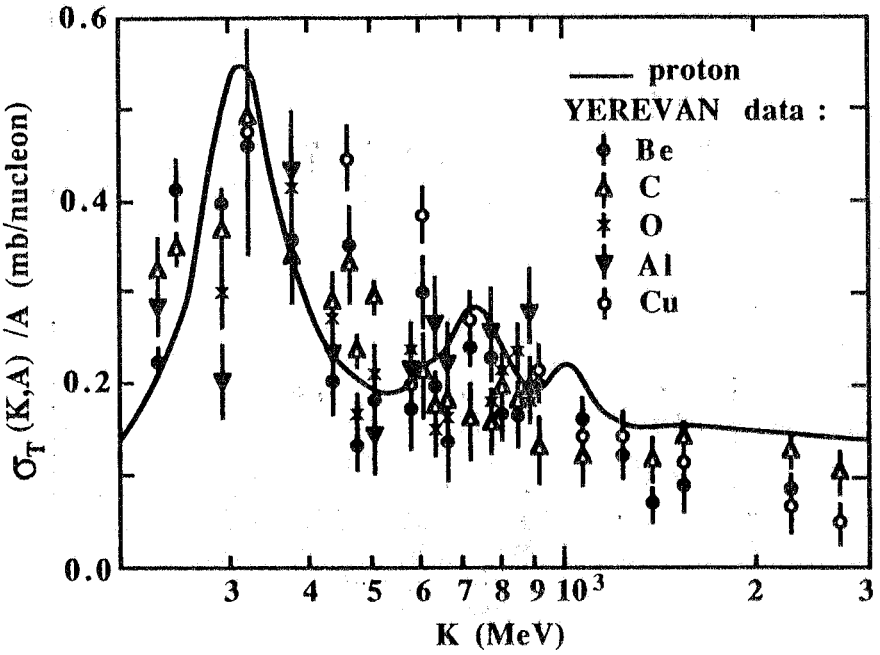

FIG. 3 - The total photonuclear cross section per nucleon, $\sigma_T(k, A)/A$, as a function of photon energy k, measured at Erevan for Be, C, O, Al and Cu.[11] The full line, shown for convenience, is relative to the proton.

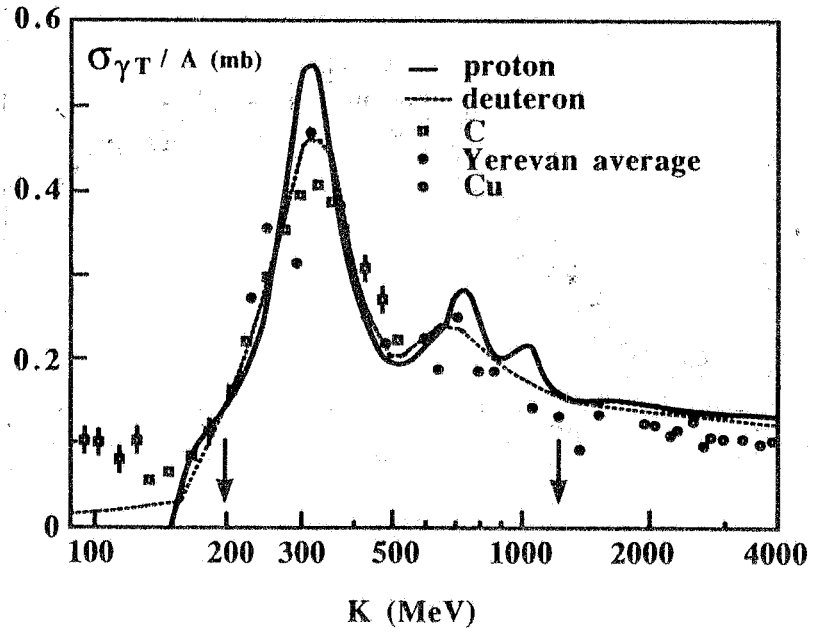

FIG. 4 - Behavior of the total photonuclear cross section per nucleon $\sigma_T(k, A)/A$ in the "Resonances" region, for the proton (full line) and various nuclei: dotted line, Deuteron; open squares, Carbon; open diamonds, Copper; full circles, average of Erevan measurement on Be, C, O, Al and Cu nuclei. The energy region covered by the jet target tagged photon beam is marked by the two vertical arrows.

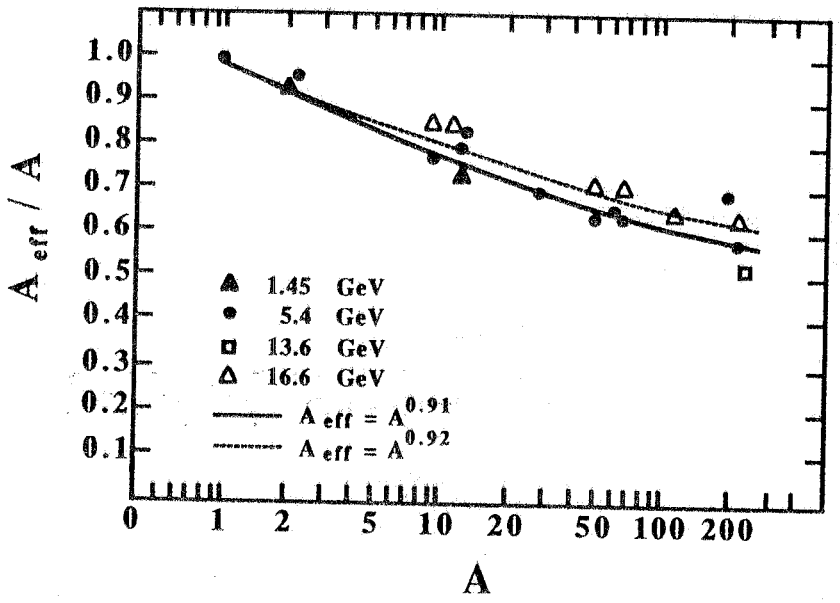

FIG. 5 - Behavior of the ratio A_{eff}/A, as a function of mass number A, deduced by measurements of total photonuclear cross sections with photons of energy from 1.5 GeV up to 16.4 GeV. The two curves refer to the behavior of $A_{eff}=A^{\alpha}$ for $\alpha=0.91$ (full curve) and $\alpha=0.92$ (dashed curve).

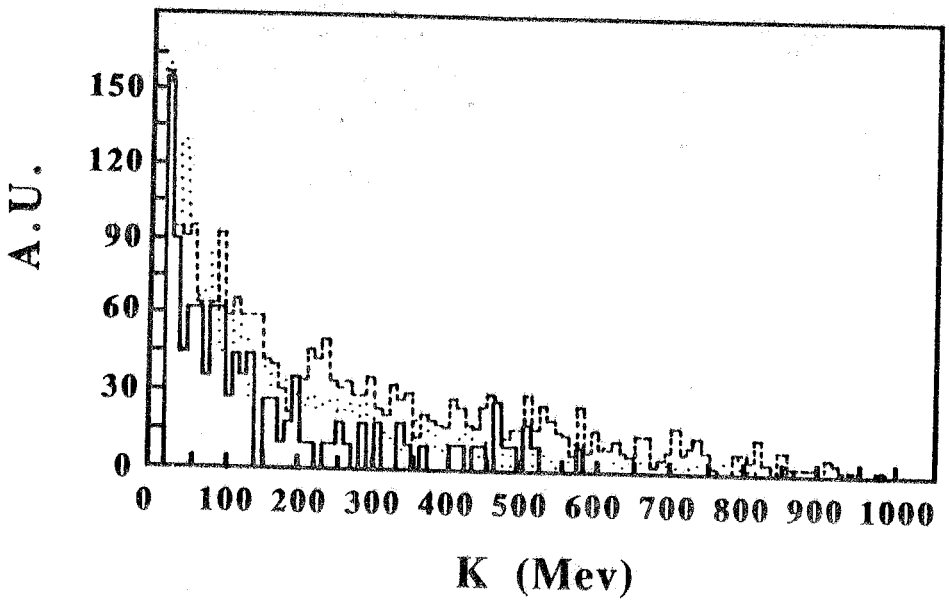

FIG. 6 - Monte Carlo calculation of the spectra of secondary photons on the detector, for a primary bremsstrahlung spectrum of 1 GeV maximum energy. Dashed curve: no magnetic field; dotted curve: magnetic field of 12 kG after the absorption target; full curve: magnetic field of 12 kG and absorption target inside the field. The absorber is Carbon of 25 cm of thickness. All spectra are normalized to the same number of incident photons on the absorber.

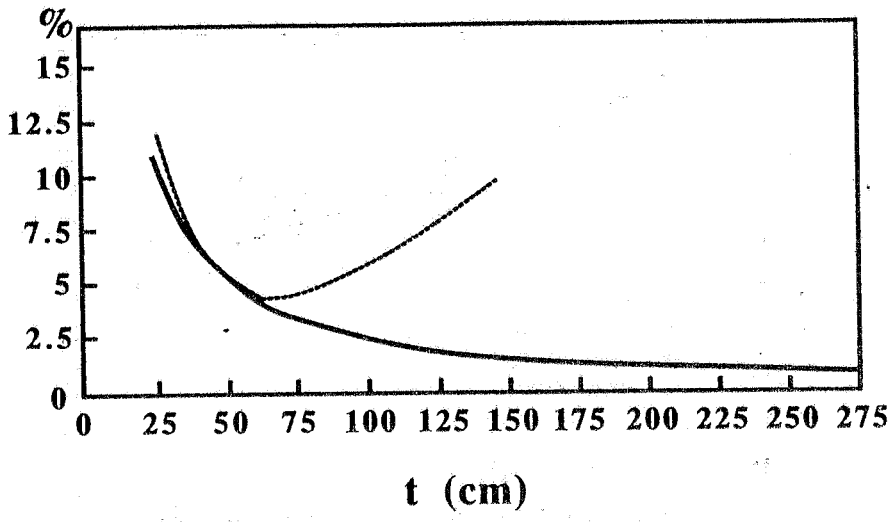

FIG. 7 - Example of the behavior of the statistical error (%) on $\sigma_T(k, A)$ as a function of the thickness t (cm) for a Be absorber, calculated from errors propagation in eq.3 in the following conditions: k=800 MeV, photon intensity ≈80 photons s^{-1} and per channel, total measurement time (with target in and target out) ≈24 hours. The full curve is for photon intensity constant on the detector; the dashed one is for constant intensity of the primary photon beam.

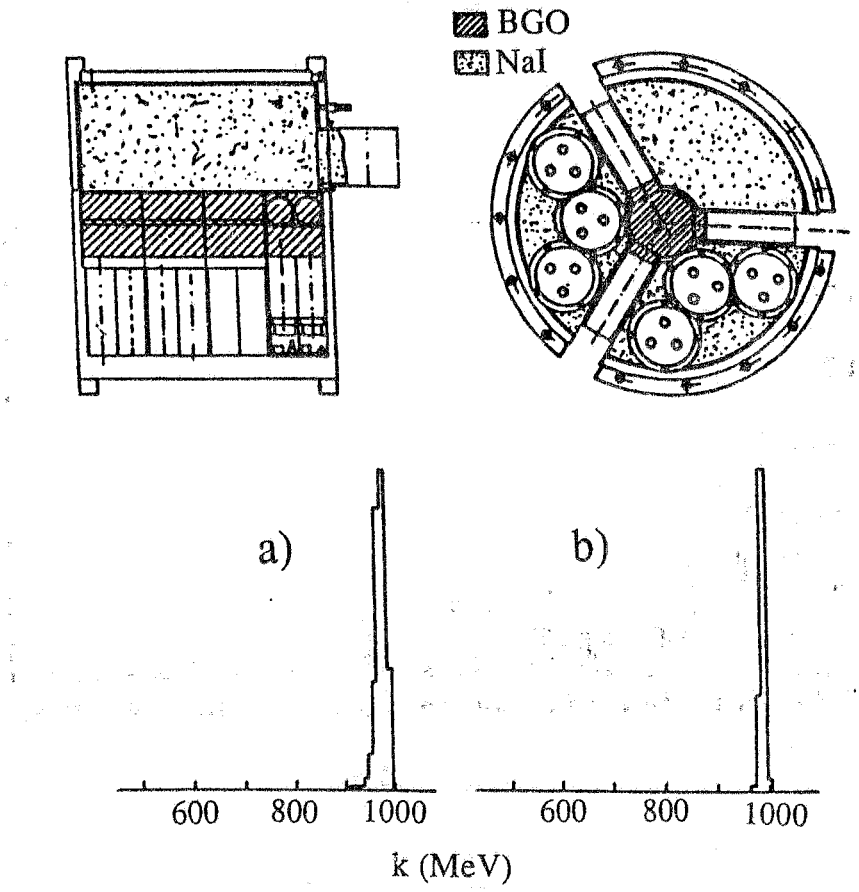

FIG. 8 - Upper figure:-lateral and front view of the BGO and NaI crystals photon spectrometer and its phototubes. Bottom figure: Monte Carlo calculated response function for 1 GeV monochromatic photons: a) without NaI in anticoincidence; b) with NaI in anticoincidence.

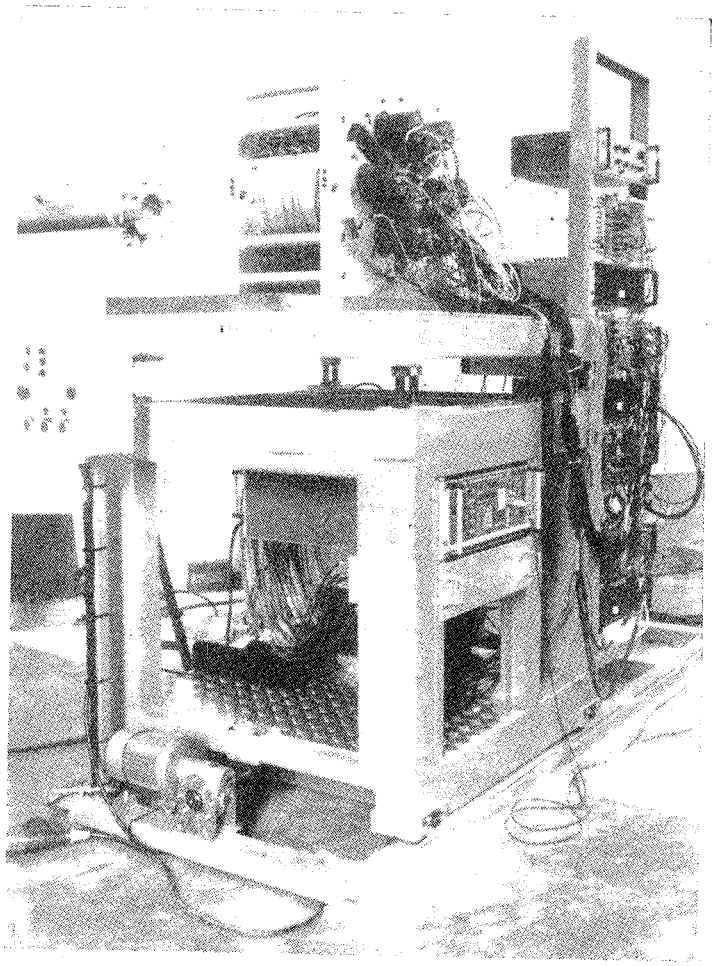

FIG. 9 - The photon spectrometer and its electronics mounted in the experimental hall, above the remotely controlled platform. The shielding has been removed. The vacuum transport tube of the photon beam is visible on the left.

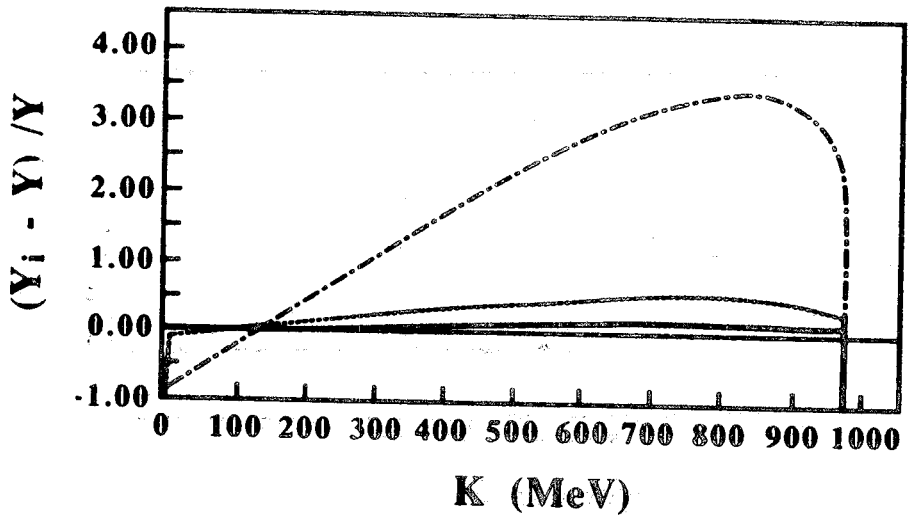

FIG. 10 - Calculated pile-up effects in the bremsstrahlung photon spectrum of maximum energy 980 MeV for the BGO spectrometer for different photon intensity (integrated from 10 MeV up to maximum energy). Dot-dashed curve: 10^6 photons/s; dashed curve: 10^5 photons/s; full curve: 4×10^4 photons/s. The ordinate gives the fractional pile-up of the spectrum.

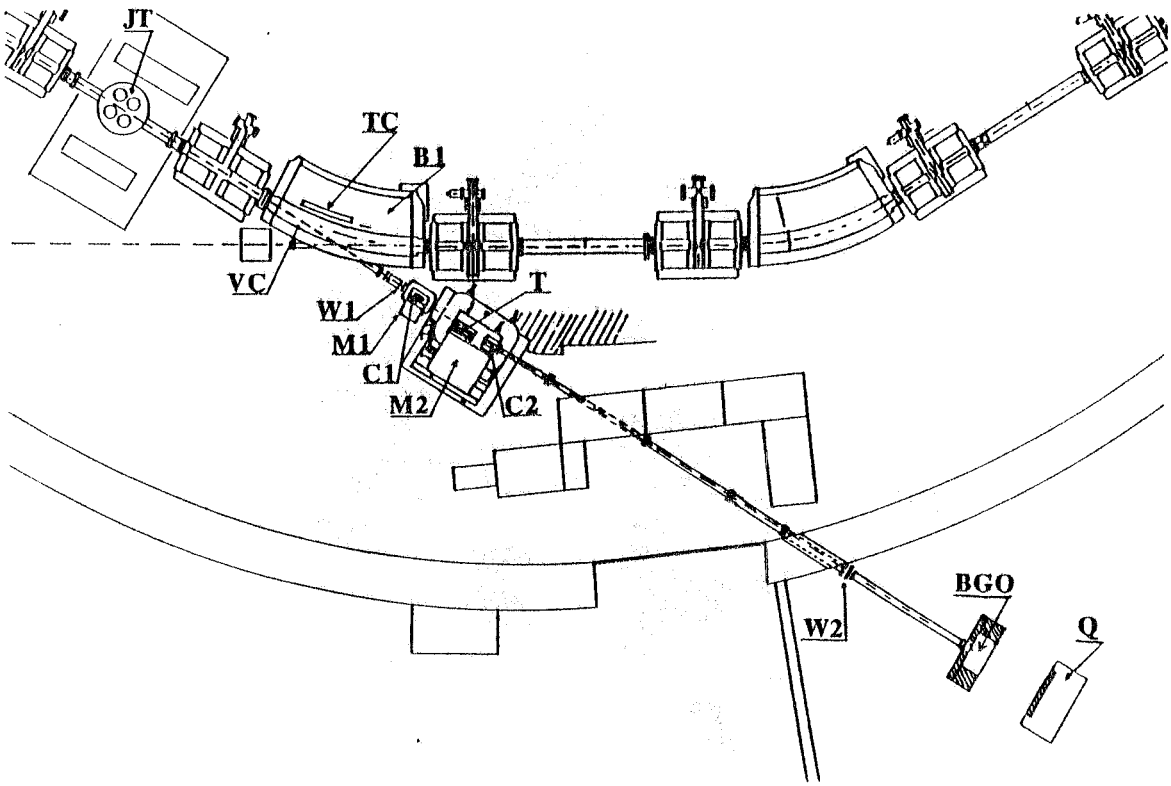

FIG. 11 - General view of the Jet Target Tagged photon facility and of the experimental set-up for the total photonuclear cross section experiment on light nuclei. JT: Jet Target; VC: vacuum chamber; W1: photon beam wire profile chamber; TC: tagging counters; B1: ADONE bending magnet; C1: photon beam collimator; M1: sweeping magnet; T: absorption target or vacuum simulator; M2: dumping magnet; C2: photon collimator; BGO: photon spectrometer; W1: photon beam wire profile chamber; Q: quantameter.

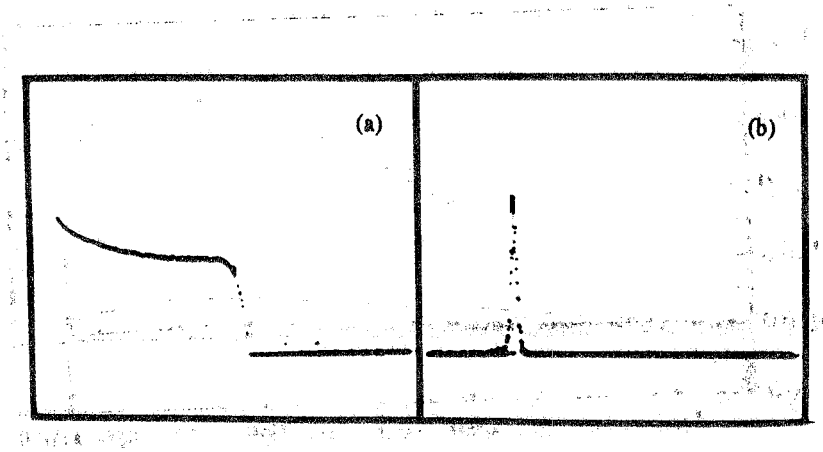

FIG. 12 - Bremsstrahlung spectrum for electron energy 1200 MeV, measured by the BGO spectrometer (a). Spectrum measured by the BGO detector in coincidence with one tagging channel (b): the FWHM is ≈3%.

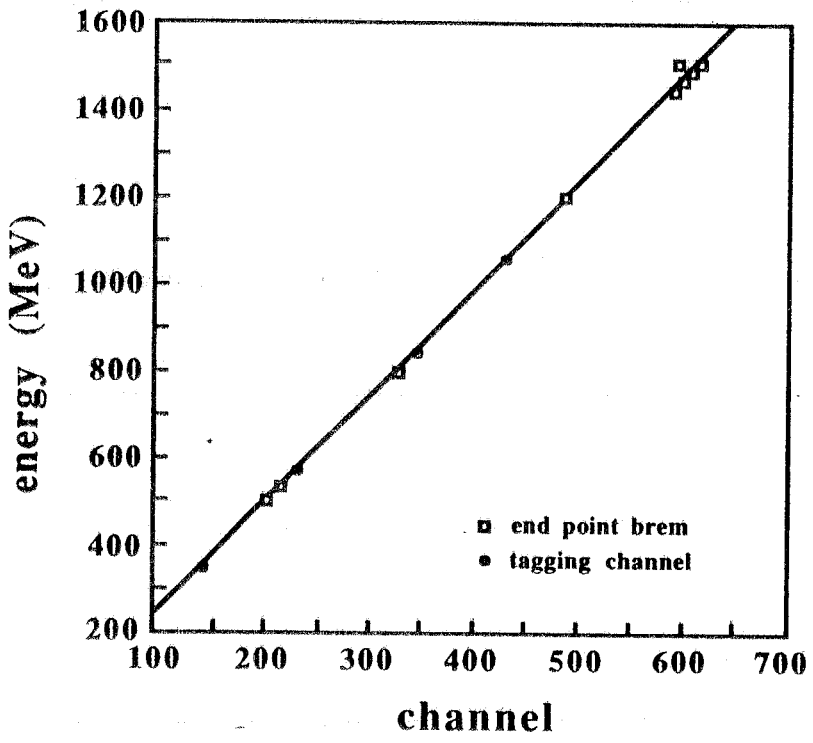

FIG. 13 - Channel-energy relation of the BGO spectrometer measured in different conditions, using the head energy of the bremsstrahlung beam (full points) and the peak position in coincidence with a selected tagging channel (open points).

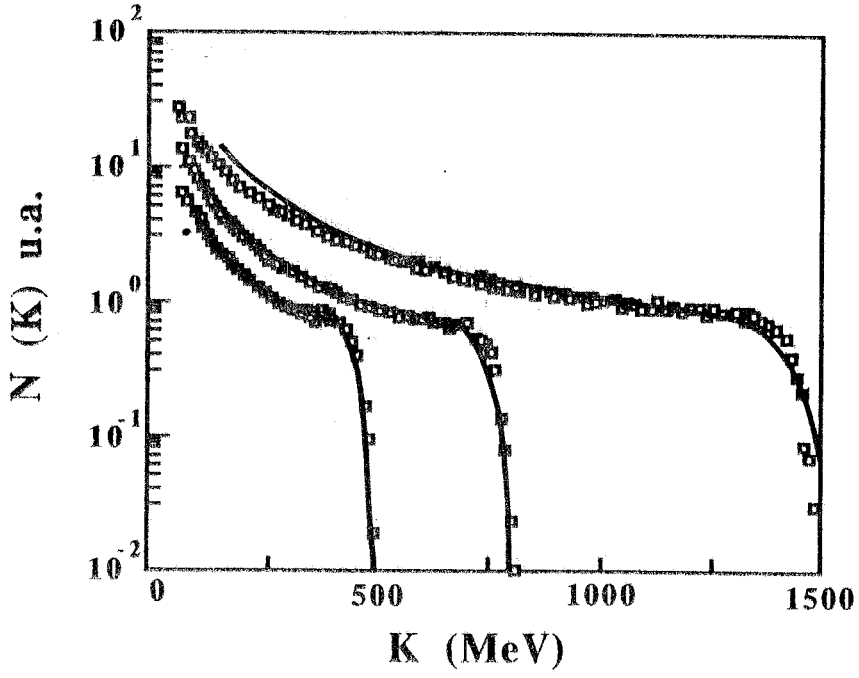

FIG. 14 - Experimental and calculated bremsstrahlung spectra, at different electron energies. The calculation are performed with a shower Monte Carlo code.

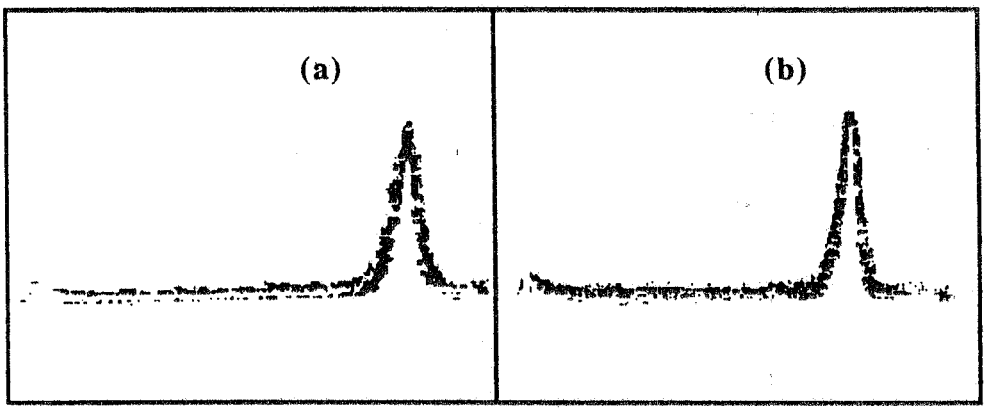

FIG. 15 - BGO spectrum in coincidence with channel ≠13 of tagging system, for electron energy 1500 MeV MeV: a) with absorber Out; b) with absorber In.

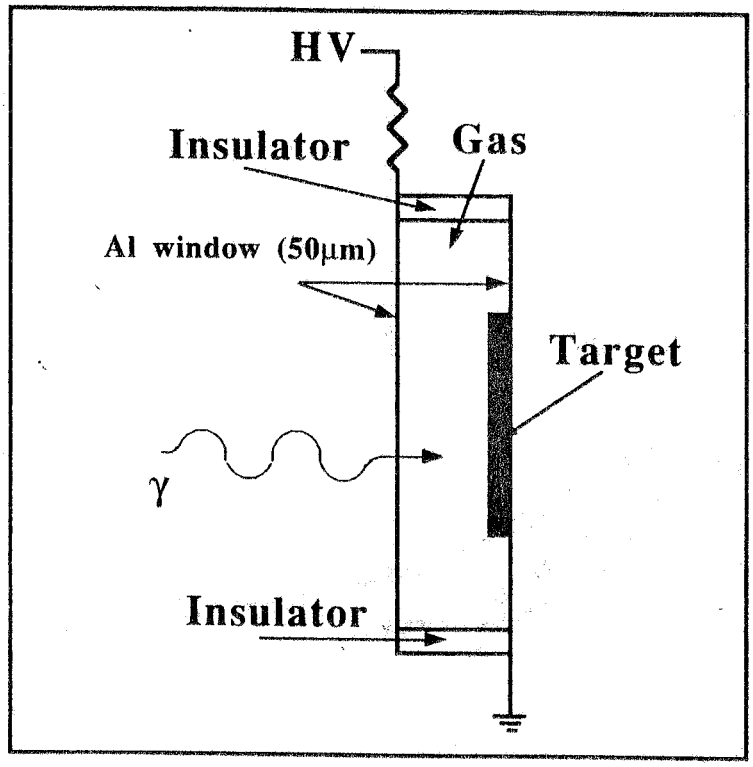

FIG. 16 - Schematic drawing of a PPAD counter.